


Journal of Life Science and Public Health (JLSPH)

Volume 1 Issue 2, (2025)

 <https://doi.org/10.69739/jlsph.v1i2.1085>

 <https://journals.stecab.com/jlsph>



Published by
Stecab Publishing

Research Article

Study of Intercellular Adhesion Protein Expression in *Staphylococcus aureus* under Treatment of Phenolic Conjugated Copper Nanoparticles

*¹Sajjad Mohsin Irayyif

About Article

Article History

Submission: September 09, 2025

Acceptance : October 14, 2025

Publication : October 20, 2025

Keywords

Biofilm, Copper nanoparticles, MIC, qPCR, *Spathodea campanulata*, *Staphylococcus aureus*

About Author

¹ Department of Medical Basic Sciences,
College of Dentistry, University of
Wasit, Wasit, Iraq

Contact @ Sajjad Mohsin Irayyif
salazawi@uowasit.edu.iq

ABSTRACT

Staphylococcus aureus is one of the most prevalent infectious organisms that contribute to morbidity and mortality worldwide. This bacterial pathogen can cause a wide range of ailments, from pneumonia and sepsis to severe skin infections. There is presently no effective immunization against *S. aureus* infections, and antibiotic resistance makes treatment more challenging. The green biosynthesis of nanoparticles (NPs) utilizing biomaterials is a recent area of interest in nanotechnology and nanoscience. The goal of this work was to create phenolic conjugated copper nanoparticles (CuNPs), a unique use of nanotechnology. The investigation was conducted to determine the antibacterial activity against *Staphylococcus aureus* after characterizing using FTIR and UV-Vis absorption spectra. We discovered a distinctive signal at 365 nm that corresponds to the phenolic extract's surface plasmon resonance (SPR). Our findings supported the green produced CuNPs' possible antibacterial function. Additionally, we observed a noteworthy 84% suppression of biofilms in comparison to the positive control, rifampicin. We discovered that the *icaA*, *icaB*, *icaC*, and *icaD* gene members were down-regulated as a percentage from the qPCR analysis. In conclusion, the environmentally friendly synthesis of CuNPs from phenolics can be a good option for clinical applications such drug delivery systems, pharmaceutical formulation, and biological applications.

Citation Style:

Irayyif, S. M. (2025). Study of Intercellular Adhesion Protein Expression in *Staphylococcus aureus* under Treatment of Phenolic Conjugated Copper Nanoparticles. *Journal of Life Science and Public Health*, 1(2), 39-47. <https://doi.org/10.69739/jlsph.v1i2.1085>



Copyright: © 2025 by the authors. Licensed Stecab Publishing, Bangladesh. This is an open-access article distributed under the terms and conditions of the [Creative Commons Attribution \(CC BY\)](https://creativecommons.org/licenses/by/4.0/) license.

1. INTRODUCTION

Staphylococcus aureus is one of the most well-known and widespread bacterial pathogens, which causing an estimated hundreds of thousands to millions of more serious, invasive infections annually globally (Klevens *et al.*, 2007; Rasigade *et al.*, 2014). It is a leading cause of cardiovascular, surgical site, prosthetic joint, nosocomial bacteremia, and various respiratory tract infections, including pneumonia. *S. aureus* infections are particularly problematic because to the high prevalence of antibiotic resistance in *S. aureus* isolates, among which methicillin-resistant *S. aureus* (MRSA) is the most significant clinically. Compared to methicillin-sensitive *S. aureus* (MSSA) infections, MRSA infections are associated with higher rates of hospitalization, death, and morbidity (Tong *et al.*, 2015).

In *S. aureus*, resistance to various antibiotics is also common. For instance, *S. aureus* is almost always resistant to conventional beta-lactam antibiotics (penicillin and its derivatives) that are sensitive to beta-lactamase (Van Hal *et al.*, 2012). Furthermore, *S. aureus* can show resistance to almost every antibiotic currently in use, often in combination. Vancomycin remains the antibiotic of last choice for MRSA infections since highly vancomycin-resistant strains (VRSA) have been identified but have not spread. Vancomycin resistance genes incur a considerably greater fitness cost, which is probably why this is the case (Kourtis *et al.*, 2019).

2. LITERATURE REVIEW

Polysaccharide intercellular adhesion (PIA), a crucial component of biofilms, is produced by proteins encoded by the genes *icaA*, *icaB*, *icaC*, and *icaD* (creating the *icaABCD* operon) in *Staphylococcus aureus* (Gajewska and Chajęcka-Wierzchowska, 2020). In addition to mediating cell-to-cell adhesion, the polysaccharide PIA is necessary for the development of biofilms, which are multicellular communities that may enhance bacterial resistance and persistence. PIA makes it easier for *S. aureus* cells to adhere to surfaces and to one another, which is crucial for the early phases of biofilm development. One of *S. aureus*'s main virulence factors is the creation of biofilms, which aids in the spread of the bacteria, persistent infections, and antibiotic resistance (Gajewska & Chajęcka-Wierzchowska, 2020).

Similar to those present in plants, phenolic compounds exhibit strong antibacterial action against strains of *Staphylococcus aureus* (*S. aureus*), even those that are resistant to antibiotics (Mahros *et al.*, 2021). These substances have the ability to break down bacterial cell walls, prevent the formation of biofilms, and even lessen resistance to antibiotics. Examples of substances that have demonstrated strong antibacterial action against *S. aureus* include hydroquinone, quercetin, and chrysin (Abdallah *et al.*, 2022). Phenolic substances have the ability to damage the bacterial cell wall, which can result in cell lysis and death. It can be challenging to treat *S. aureus* biofilms with traditional antibiotics. Biofilm production can be inhibited by some phenolic chemicals, such as those present in olive oil (Alghamdi *et al.*, 2023). Because nanoparticles (NP) have special qualities and are used in a variety of industries, nanotechnology is growing in popularity (Hakim *et al.*, 2021). They make good research subjects for the battle against infectious diseases because

the medical community has recently become considerably more aware of NP's antibacterial and antiviral characteristics (Hajmohammadi *et al.*, 2021). NPs can solve a wide range of scientific and technological issues. Because of their antiviral and antibacterial qualities, NPs have recently attracted a lot of interest from the medical community. As such, they are of great interest for research on infectious disease prevention and control (Ordeghan *et al.*, 2022). The synthesis method utilized to produce the NPs has an impact on the morphology, size, and form of the molecules. This field of study is difficult because of the fast oxidation (Król *et al.*, 2017). Despite much research, little has been done about copper, despite its low cost. Compared to other noble metals, copper (Cu) is abundant and antimicrobial in nature (Motallaei *et al.*, 2021).

The environmentally friendly production of nanomaterials without the use of hazardous chemicals has been a major focus of nanoscience research in recent decades. This promotes the development of environmentally friendly practices (Pérez-Alvarez *et al.*, 2021). Metallic nanoparticles can be produced using microorganisms and plant extracts, with the active biological component serving as a cost-effective reducing agent and capping agent (Baetke *et al.*, 2015). As a result, experimental investigations do not require excessive pressure or energy, resulting in energy-efficient and environmentally safe operations. One of the most important tactics in green synthesis to create stable nanoparticles is to optimize the reaction conditions (Moghadam *et al.*, 2021). The efficacy of nanoparticles in a variety of applications, such as targeted therapy and drug administration, can be greatly increased by conjugating them to pharmaceuticals or other compounds. Techniques like enhanced medication encapsulation, solubility, and bioavailability are used to accomplish this. The orientation and immobilization of the conjugated molecules on the nanoparticle surface are influenced by various conjugation strategies, including covalent binding and adsorption, which affects the overall effectiveness of the particle (Juan *et al.*, 2020). Examining the potential for creating CuNPs using phenolic compounds isolated from *Spathodea campanulata* was the aim of this study. The green synthesised CuNPs were used to test for antibacterial and anti-biofilm properties against the human skin pathogen *Staphylococcus aureus*. Real-time PCR expression profiling of the proteins linked to biofilms confirmed the antibacterial properties.

3. METHODOLOGY

3.1. Extraction of phenolic compounds

Spathodea campanulata petals weighing 500gm were gathered at the university campus in Thanjavur, Karnataka, Country. After completely washing and homogenizing each petal in a mortar, several solvents, including 100% chloroform, 100% ethyl acetate, and 100% methanol were applied for extraction. After mixing the ingredients, they were incubated at room temperature with continuous stirring for three days. After that, the contents were filtered, and the volume of the filtrate was recorded. After letting the filtrate drain at room temperature, the weight of the residual residue was noted. For use in subsequent investigations, the dried extract was reconstituted with the appropriate solvent at a ratio of 1 mg/ml.



3.2. Preliminary screening and estimation of total polyphenol content

About 0.1ml of each extract was added with few drops of ferric chloride (FeCl_3 , 5%) and observed for a blue violet or purple colour, which indicates the presence of phenol (Kancherla *et al.*, 2019). Using the FC reagent, the total phenol content of *Spathodea campanulata* extracts was ascertained using the methodology outlined by McDonald *et al.*, (2001). About 5mL of the Folin-Ciocalteu reagent (1:10) and 4ml of sodium carbonate (1M) are added to 0.5ml of each extract (1mg/ml). A spectrophotometer is used to detect the optical density at 765nm following a 15-minute incubation period at room temperature. A standard curve is drawn using the Gallic acid (in methanol) as standard used to find the concentration of the extracts. The total phenol content of the extracts is expressed in terms of gallic acid equivalents per gram of extract (mg GAE / g).

3.3. Green synthesis of copper nanoparticles (CuNPs)

After adding roughly 10mg of methanolic extract, which was discovered to be high in polyphenols (PE), to 100 ml of deionized water, an equal volume of 3mM copper sulphate solution was added while being continuously stirred (800rpm). For 24 to 48 hours, the contents are agitated at 40°C in the dark. The reaction was halted when the colour changed from yellowish to reddish brown, confirming the synthesis of CuNPs. To pellet down the produced CuNPs, the mixture was centrifuged for 15 minutes at 13,000rpm. After being twice cleaned with deionized water, the resulting pellet was dried in a hot air oven. Characterization studies were conducted using the produced CuNPs (Bakhshi *et al.*, 2022). The particulates were evaluated for antibacterial activity against *Staphylococcus aureus* after being characterized.

3.4. Characterization of synthesized CuNPs

A DLS model SZ-100 was used to evaluate the size distribution and polydispersity index (PDI). A UV-Vis spectrophotometer model (1800, Shimadzu) was used to measure the absorbance spectra across the 200–800 nm wavelength range. After the green CuNPs were freeze-dried, the biomolecules found in the plant extracts surrounding the synthesized green CuNPs were then categorized using a FTIR spectrometer (500–4000 cm^{-1}). For the morphological analysis, SEM was employed. The morphology of the CuNPs was analyzed to see if any aggregates or agglomerates had developed.

3.5. Bacterial strains

We got strains of *Staphylococcus aureus* from the In search Biotech facility in India. Chemicals, nutrient broth, Rifampicin (HiMedia) were acquired from HiMedia Ltd. in India. The bacteria were kept as pure stock after being resurrected and maintained as pure culture in nutrient broth for 12 to 18 hours at 37°C.

3.6. Antibacterial activity tests

The antibacterial activity of GCuNPs was screened using the agar well diffusion method. After being inoculated into a nutrient broth medium, a loopful of *S. aureus* overnight culture was cultured for the entire night at 37°C. The inoculum consisted of cell suspensions that had been roughly adjusted. For the pour

plate, roughly 100 μl of culture (1×10^8 CFU/ml) was employed. After cutting wells at equal intervals, 20 μl of GCuNPs and a positive control (Rifampicin 5mg/ml) were added. Tests were conducted using GCuNPs at different concentrations. The plates were incubated in an aerobic environment for 24hr at 37°C. After incubation, the zone of inhibition's diameter (measured in millimeters) was noted.

3.7. Minimum inhibitory concentration

With minor adjustments, the MIC of the synthesized NPS was calculated in accordance with Sudhakar and Raman, (2020) description. GCuNPs at a range of concentrations (10, 20, 40, 80, and 100 $\mu\text{g}/\text{ml}$) were made using de-ionized water. Each tube with the numbers 1 through 8 received 1ml of broth. About 20 μl of culture, inoculated into all the tubes. Rifampicin was used as a positive control. Each tube labelled was added with 50 μl of respective treatment. After carefully mixing the ingredients, they are incubated for 12 to 18 hours at 37°C. After incubation, the OD at 650nm was recorded to determine whether growth was occurring or not.

3.8. Biofilm inhibition assay

Green nanoparticles were found to be beneficial in preventing the formation of biofilms, but they were somewhat modified from Sudhakar and Raman (2020). In short, nutritional broth containing glucose solution was used to dilute overnight cultures (1: 100). The labelled wells were seeded with 10 μl of isolate and filled with 170 μl of nutritional broth. As in the preceding section, wells labelled treatments were treated with about 20 μl of the nanoparticles at different concentrations, while well 1 served as the negative control (untreated) and well 2 as the positive control. The plate was incubated at 37°C for the entire night. After that, 200 μl of PBS (pH7.4) was used to wash the wells three times. After cleaning, the plates were allowed to air dry before being dyed for 15 minutes with 2% crystal violet. After solubilizing the crystal violet with 200 μl of ethanol:acetone (80:20) in the wells, the plates were placed in a plate reader (Genetix, Germany) to measure the absorbance at 590nm. The formula for calculating biofilm inhibition is as follows: % biofilm inhibition = $1 - (\text{OD}_{590} \text{ of cells} / \text{OD}_{590} \text{ of control cells}) \times 100$.

3.9. RNA extraction

3.9.1. Treatment

The tubes used in the previous MIC section following recording the absorbance, were used for RNA extraction and qPCR.

3.9.2. RNA extraction

The RNA extraction process was carried out according to the directions in the manual. The resulting supernatant was discarded after the cultures (1×10^8 bacteria) were centrifuged at 8000rpm for 5min at 4°C. After adding 500 μl of Buffer RLT to the pellet, it was vigorously vortexed for 5–10 seconds. After about ten seconds of full-speed centrifugation, the contents were gathered in a fresh tube. An equivalent volume of 70% ethanol was pipetted in and thoroughly mixed. The 700 μl of collected lysate was placed in a 2 ml collection tube and placed into the RNeasy spin column. The contents were centrifuged for 15



seconds at a speed of about 8000rpm, and the flow was then disposed of. After discarding the flow-through, 500µl of Buffer RPE was centrifuged for 15 seconds at 8000rpm to wash the RNeasy spin column. The previous technique was repeated twice to clear the membrane. Before the column was put in a new collection tube, about 50µl of molecular grade water was added.

3.9.3. Reverse transcription (RT) PCR: cDNA synthesis

The cDNA was produced using the SuperScript TMII Reverse Transcriptase, 200U/l (HiMedia) RT PCR kit. In summary, roughly 2µg of the RNA obtained in the previous phase was used to start the first reaction. A total of 1.54µg/ml of RNA was

recovered. Thus, 1µl of RT enzyme, 1.31µl of total RNA, and random primers were utilized.

3.9.4. Real-time PCR

The real-time primers (Table 1) were designed using Primer3 software and then acquired from Sigma-Aldrich. The real-time PCR experiment was then carried out using the iQTM SYBR Green Supermix (HiMedia) in compliance with the findings of Kalužna *et al.* (2016). Primers (600nM) and 1µl of the RT products were utilized in the PCR experiment. Each reaction was carried out in triplicate and in tandem with its matching negative control in order to confirm the positive amplification.

Table 1. List of primers for intercellular adhesion gene members (ica) genes

Gene	Sequence (5'-3')	Tm	GC%	Product size
icaA	F	GAGGTAAAGCCAACGCACTC	58.76	151
	R	CCTGTAACCGCACCAAGTTT	58.73	
icaB	F	ACCCAACGCTAAAATCATCG	58.99	211
	R	GCGAAAATGCCCATAGTTTC	59.05	
icaC	F	ATACCGGCGACTGGGTTTAT	59.05	152
	R	TTGCAAATCGTGGGTATGTGT	58.99	
icaD	F	CTTGGGTATTTGCACGCATT	63.24	231
	R	GCAATATCATGCCGACACCT	58.6	
recA	F	ATCTCCGTCAATCTCCGCAC	59	152
	R	ACGCGCTGAACAAAAGGTTC	59.97	

3.9.5. Expression of drug target gene members

Using the Corbett Research cyclor (Bio-Rad), both the control and treatment were quantified. Primer concentrations of around 600nM for icaA, icaB, icaB and icaD were used in the amplification protocol. About 40 cycles of the program were run utilizing the RNA products at 92°C for 60s, 62°C for 45s, and with an elongation at 72°C for 50s. The housekeeping gene recA was amplified together with the pertinent genes of interest in order to detect mRNA expression. The $\Delta\Delta C_t$ method was used to compare the relative levels of mRNA in the test samples and the control.

3.10. Statistical analysis

For every experiment, three duplicates were conducted. When applicable, data were subjected to one-way analysis of variance (ANOVA), and Tukeys test differences across samples were confirmed at $P < 0.05$ (Al-Gharban & Al-Tae, 2016; Ajaj *et al.*, 2021).

4. RESULTS AND DISCUSSION

All of the three extracts showed positive for phenolic content from the ferric chloride test. Among the three extracts, methanolic extract showed rich polyphenol content when compared to the other two extracts. The extract concentrations were calculated using the gallic acid as a reference with the linear regression equation ($y = 6.2134x + 0.0$; $R^2 = 0.9934$). The results are shown in Figures 1 and 2 as mg GAE / g DE and mg

EA / g DE. Methanolic extract was found to be 12.31 ± 0.45 mg GAE. Chloroform and ethyl acetate showed 5.64 ± 0.21 mg and 6.57 ± 0.25 mg GAE respectively.

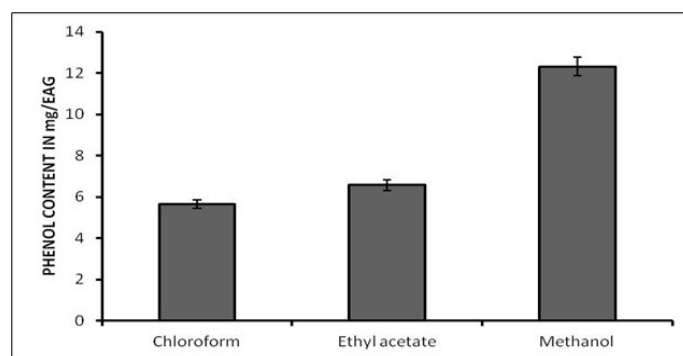


Figure 1. Total Polyphenol content. Standard regression equation of gallic acid ($y = 6.2134x + 0.0$; $R^2 = 0.9934$)

4.1. UV spectroscopy

A UV-visible spectrophotometer was used to assess the green synthesised CuNPs' surface plasmon resonance (SPR) properties. The characteristic peak at specific light wavelengths is produced by the SPR of the electrons on a nanoparticle's surface. PCuNPs' UV-Vis spectra revealed an SPR with a characteristic peak at 365nm (Figure). Phenol peak can be seen at 280nm in the graph (A) (Hajizadeh *et al.*, 2022).



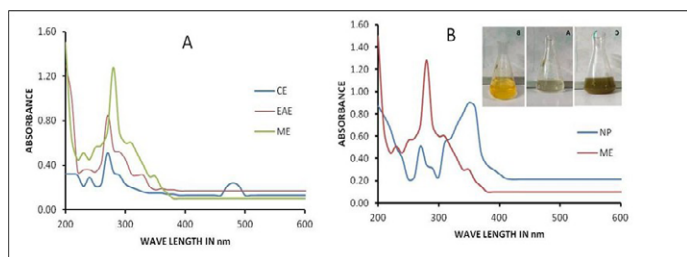


Figure 2. Image of the UV spectra obtained for the GCuNPs

The Fourier transform is used in FTIR spectroscopy to determine the frequency of molecule vibration. The figure shows the CuNPs' infrared spectra in the 4000-400 cm^{-1} frequency band using phenol extract. Free hydroxyl groups and their intra- and intermolecular H-bonds were the cause of the prominent peak in the phenol extract spectra at 3410 cm^{-1} . The aromatic stretching frequencies for C = O and C = C were linked to sharp peaks at 1702.34 and 1034.23. A 621 cm^{-1} absorption band was visible in the monoclinic phase of CuNPs (Figure 3). Studies also reported of the similar peaks with phenol (Hajizadeh *et al.*, 2022).

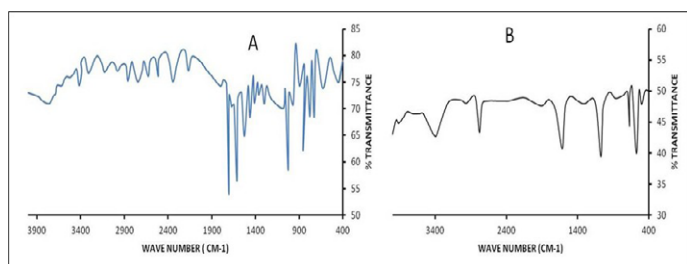


Figure 3. FTIR spectra of CuNPs (B) formed and the phenol extract (A) spectra from 400 to 4000 cm^{-1}

4.2. NTA analysis

Using dynamic light scattering spectroscopy (DLS), the size and charge of particles in an aqueous solution were examined. The DLS study's findings showed that the CuNPs made from the phenolic had an average particle size of 80 nm. Particle sizes less than 100 nm have greater potential in biomedical applications since the kind of interaction that occurs between nanoparticles and cells is highly dependent on the size of the nanoparticle. The CuNPs' charge, or Zeta potential, was evaluated to investigate their potential interaction with other macromolecules. The results showed that the CuNPs generated had a charge of -18.4mV. Previous studies on the charge as well as particle size of CuNPs (Chung *et al.*, 2016) corroborate our findings.

4.3. Agar well diffusion assay and MIC

The results of the inhibition zone showed that CuNPs had more antibacterial activity than both the positive control and the control. Comparing the NPs to the positive control, the zone of inhibition was determined to be 14mm. 12mm (10 mg/ml) was the positive control (Figure 5). CuNPs exhibited MIC of 8.4 ± 0.191 at 1mg/ml (positive control; 5.2 ± 0.54 at 0.1mg/ml).

4.4. Effect on biofilm formation

Our investigation assessed the anti-biofilm activity in vitro in a

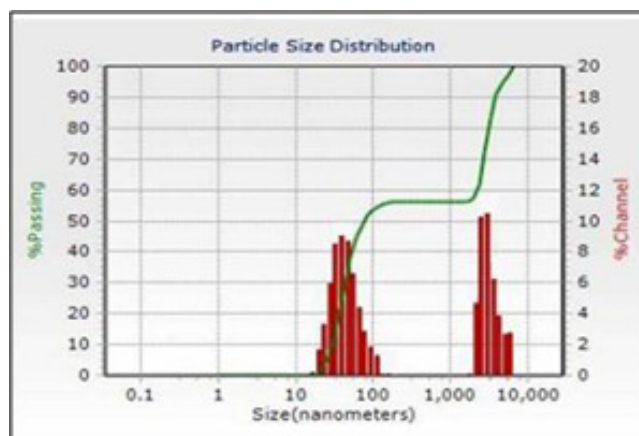


Figure 4. DLS analysis of synthesized CuNPs

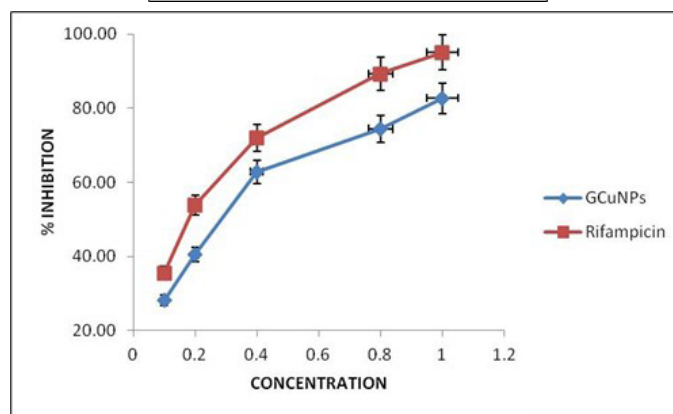
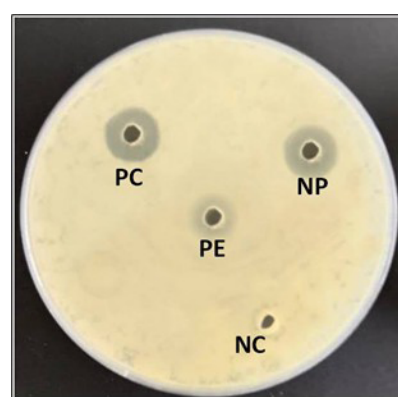


Figure 5. Left represent Plate showing the zone of inhibition (Agar well diffusion method) Right: Graph depicting inhibition of isolates using broth dilution method.

dose-dependent fashion. Compared to the experiment's control, we discovered that CuNPs prevented *Staphylococcus aureus* from forming biofilms (Figure 6). All of the GCuNPs displayed a good MIC value when the MICs of biofilm inhibition were represented in terms of IC50. At 0.1 and 1mg/ml, the synthesized CuNPs demonstrated a 42 and 97% suppression of biofilm, respectively. Our CuNPs at the same concentration demonstrated 97% biofilm inhibition, which is significant ($P < 0.05$), while the positive control showed 98% at 1 mg/ml. Its activity was assumed to be zero, and the control OD was determined to be 1.103 ± 0.43 .



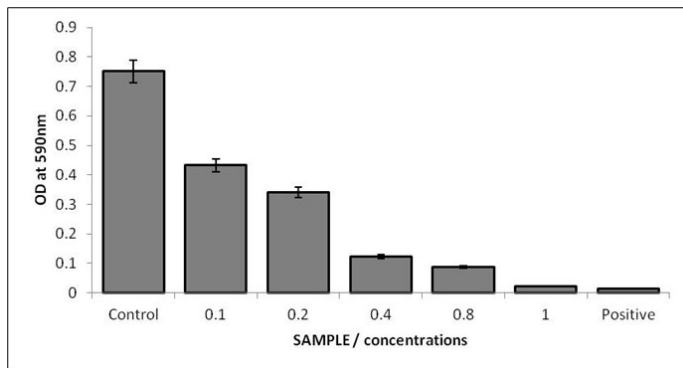


Figure 6. histogram showing the biofilm inhibition of CuNPs at different concentrations

4.5. Gene expression studies

According to the qPCR analysis, when compared to the positive control, all the four gene members were found to be down-regulated upon treatment with GCuNPs ($P < 0.05$). Each gene member's expression was expressed as a ratio of that gene's relative expression to the control gene. According to the real-time expression profile, we discovered that the *icaA*, *icaB*, *icaC* and *icaD* were 35, 16, 5 and 25% downregulated respectively. On the other hand, the positive control showed 42, 32, 12 and 35% downregulated respectively for *icaA*, *icaB*, *icaC* and *icaD*.

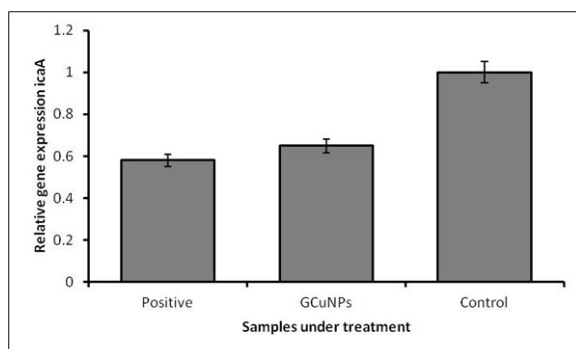


Figure 7. Histogram showing the relative gene expression of *icaA* expression

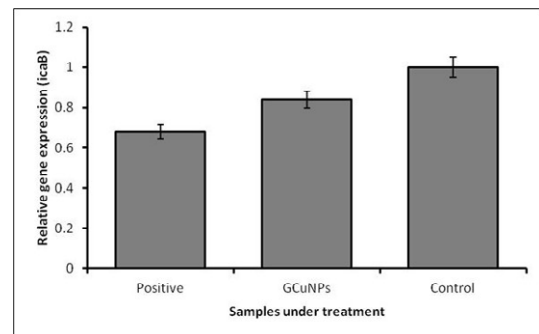


Figure 8. Histogram showing the *icaB* expression

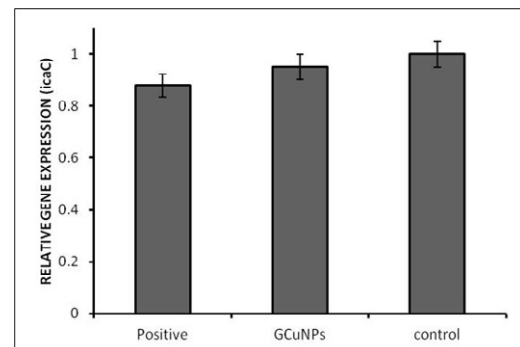


Figure 9. Histogram showing the gene expression of *icaC* expression

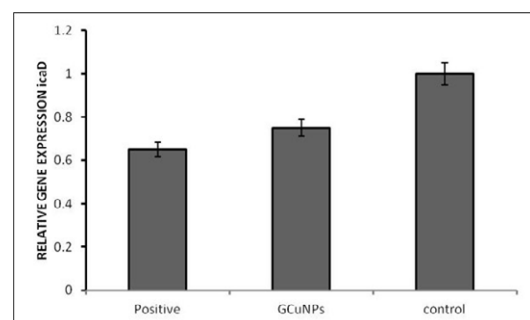


Figure 10. Histogram showing the gene expression of *icaD* expression

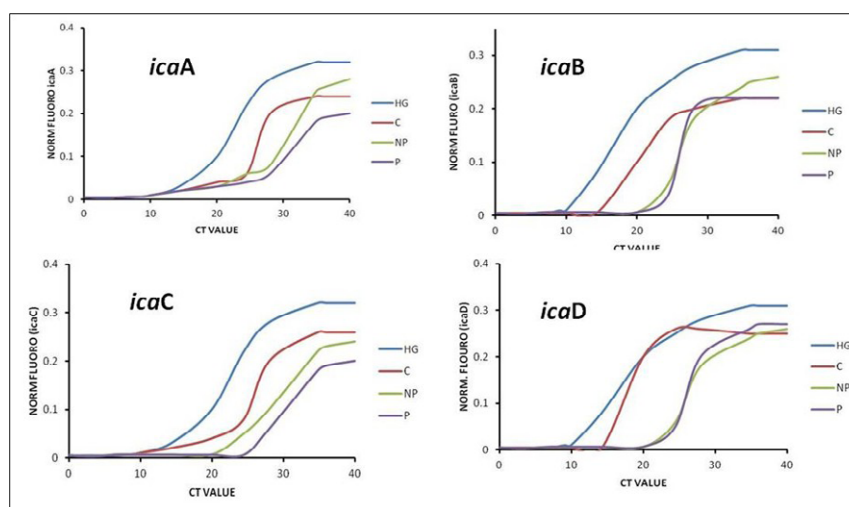


Figure 11. CT curves showing the gene expression of *icaA*, *icaB*, *icaC* and *icaD* expression



4.6. Discussion

The green synthesized CuNPs were characterized and because of their inherent antibacterial qualities, high level of efficacy, low toxicity, and capacity to stabilize CuNPs, plant extracts or green products are preferable. Their use serves as an environmentally friendly NP synthesis technique. Our findings indicate that phenolic compounds have a lot of promise for the commercial synthesis of CuNPs. Copper nanoparticles were reported to exhibit a peak at 385 nm (Hajizadeh *et al.*, 2022). The UV spectra of CuNPs at approximately 403 nm were published in studies conducted by Jain and Mehata (2017). When *Ocimum sanctum* leaf extract was used to analyze manufactured Cu NPs, a similar outcome was obtained (Jain & Mehata, 2017). Since the size of the NPs essentially determines the surface plasmon absorbance, each researcher reports a different value for NPs made with various plant extracts. Copper nanoparticles were coupled to isolated phenolic compounds. Our investigation revealed that the MIC value was significantly significant when compared to previous reports. A significant MIC of 5.65 ± 0.213 (1 mg/ml) was discovered. Our research fully supports the findings of Veiga *et al.* (2017) and Seidel *et al.* (2008).

Additionally, our biofilm results are consistent with research on motility. When compared to the positive control (74%), GCuNPs demonstrated a 92% decrease in the number of colonies at 1 mg/ml. Similar reports were seen wherein extracts derived copper nanoparticles showed potent MBC activity (Hajizadeh *et al.*, 2022). Studies done by Murthy *et al.* (2020) stated of the role of green synthesized CuNPs as antibiofilm in nature. We found a significant percent inhibition via broth dilution ($P < 0.05$). Our green synthesized NPs showed 82% inhibition at 1mg/ml which is highly significant to the positive control (95%). Many transcriptomics reports examined virulence genes and biofilms. Attachment to surfaces is the foremost in the production of *S. aureus* biofilm, which is controlled by the regulation of various microbial surface components. The synthesis of polymeric intercellular adhesion protein is initiated upon recognition of these molecules. This protein, which is encoded by *ica* Operon (*icaABCD*), regulates cell-to-cell adhesion. Fibronectin-binding proteins, clumping factors, and biofilm-binding proteins mediate this production (Boles *et al.*, 2010). Research on adhesion genes and *icaAD* has shown that these four elements are crucial for biofilm formation. We can prevent, manage, and treat infections in the future by being aware of the phenotypic and genetic traits of biofilms (Goudarzi *et al.*, 2019). Through gene expression investigations, we examined the significant function of the virulence genes (*icaA*, *icaB*, *icaC*, and *icaD*). Our goal was to find out how the four genes described above were regulated when GCuNPs were present. We can state with confidence that our study is consistent with other earlier publications. Comparing the gene members to the positive control, all of them showed under expression. Remarkably, we did not see any significant down-regulation with *icaC*. To validate these findings, more research must be conducted.

5. CONCLUSION

Although CuNPs were previously synthesized using phenolic compounds such as gallic acid, this study offers a novel way to assess antibacterial efficacy against *Staphylococcus aureus*.

The stability of CuNPs in future applications is revealed by characterization tools. CuNPs are expected to be used in drug delivery, therapeutic formulations and biological applications in the future because of their ecologically favorable biosynthetic production from natural resources. Target modification, efflux pumps, and enzymatic inactivation are some of the ways that *Staphylococcus*, and especially *S. aureus*, can become resistant to multiple antibiotics. Methicillin-resistant *S. aureus* (MRSA) and other resistant strains can cause serious infections in healthcare settings; hence this resistance is a serious concern. Promising approaches to address the increasing issue of antibiotic resistance in *Staphylococcus aureus*, especially Methicillin-resistant *Staphylococcus aureus* (MRSA), are provided by nanotechnology. By focusing on infection areas and enhancing treatment results, nanoparticles (NPs) can be employed as antibacterial agents or drug delivery systems. As new pathogen strains and disease-causing organisms emerge, the effectiveness of existing medicines and the concept of utilizing antibiotics to combat diseases is rapidly declining. A novel approach to treating biofilms and germs resistant to traditional medical treatments is offered by high throughput nanobiotechnology-tailored antimicrobials. The current study aims in using phenolic conjugated CuNPs to stop the formation of biofilms for therapeutic treatments, which offer a novel way to effectively treat a range of infectious diseases caused by harmful bacteria.

REFERENCES

- Abdallah, H. M., Al Naiemi, N., Elsohaby, I., Mahmoud, A. F., Salem, G. A., & Vandenbroucke-Grauls, C. M. J. E. (2022). Prevalence of extended-spectrum β -lactamase-producing Enterobacterales in retail sheep meat from Zagazig city, Egypt. *BMC veterinary research*, 18(1), 191.
- Ajaj, E. A., Mohammad, H. A., & Gharban, H. A. (2021). First molecular confirmation of *Coenurus cerebralis* in sheep and goats with neurological behaviors in Iraq. *Veterinary World*, 14(6), 1420-1425.
- Al-Gharban, H. A., & Al-Taei, H. S. (2016). Seroclinical diagnosis of *Anaplasma marginale* bacteria in carrier arabian one-humped camels. *Basrah Journal of veterinary Research*, 15(2) 346-359.
- Alghamdi, B. A., Al-Johani, I., Al-Shamrani, J. M., Alshamrani, H. M., Al-Otaibi, B. G., Almazmomi, K., & Yusof, N. Y. (2023). Antimicrobial resistance in methicillin-resistant *Staphylococcus aureus*. *Saudi journal of biological sciences*, 30(4), 103604.
- Baetke, S. C., Lammers, T. G. G. M., & Kiessling, F. (2015). Applications of nanoparticles for diagnosis and therapy of cancer. *The British journal of radiology*, 88(1054), 20150207.
- Boles, B. R., Thoendel, M., Roth, A. J., & Horswill, A. R. (2010). Identification of genes involved in polysaccharide-independent *Staphylococcus aureus* biofilm formation. *PLoS one*, 5(4), e10146.



- Chung, I. M., Park, I., Seung-Hyun, K., Thiruvengadam, M., & Rajakumar, G. (2016). Plant-mediated synthesis of silver nanoparticles: their characteristic properties and therapeutic applications. *Nanoscale research letters*, 11(1), 40.
- Gajewska, J., & Chajęcka-Wierzchowska, W. (2020). Biofilm formation ability and presence of adhesion genes among coagulase-negative and coagulase-positive staphylococci isolates from raw cow's milk. *Pathogens*, 9(8), 654.
- Goudarzi, M., Mohammadi, A., Amirpour, A., Fazeli, M., Nasiri, M. J., Hashemi, A., & Goudarzi, H. (2019). Genetic diversity and biofilm formation analysis of *Staphylococcus aureus* causing urinary tract infections in Tehran, Iran. *The Journal of Infection in Developing Countries*, 13(09), 777-785.
- Hajizadeh, Y. S., Harzandi, N., Babapour, E., Yazdani, M., & Ranjbar, R. (2022). Green synthesis and characterization of copper nanoparticles using Iranian propolis extracts. *Advances in Materials Science and Engineering*, 2022(1), 8100440.
- Hajmohammadi, E., Molaei, T., Mowlaei, S. H., Alam, M., Abbasi, K., Khayatan, D., & Tebyanian, H. (2021). Sonodynamic therapy and common head and neck cancers: in vitro and in vivo studies. *European Review for Medical and Pharmacological Sciences*, 25(16).
- Hakim, L. K., Yazdani, M., Alam, M., Abbasi, K., Tebyanian, H., Tahmasebi, E., & Yazdani, A. (2021). Biocompatible and biomaterials application in drug delivery system in oral cavity. *Evidence-Based Complementary and Alternative Medicine*, 2021(1), 9011226.
- Jain, S., & Mehata, M. S. (2017). Medicinal plant leaf extract and pure flavonoid mediated green synthesis of silver nanoparticles and their enhanced antibacterial property. *Scientific reports*, 7(1), 15867.
- Juan, A., Cimas, F. J., Bravo, I., Pandiella, A., Ocaña, A., & Alonso-Moreno, C. (2020). An overview of antibody conjugated polymeric nanoparticles for breast cancer therapy. *Pharmaceutics*, 12(9), 802.
- Kancherla, N., Dhakshinamoorthi, A., Chitra, K., & Komaram, R. B. (2019). Preliminary analysis of phytoconstituents and evaluation of anthelmintic property of *Cayratia auriculata* (in vitro). *Maedica*, 14(4), 350-356.
- Kałużna, M., Albuquerque, P., Tavares, F., Sobiczewski, P., & Puławska, J. (2016). Development of SCAR markers for rapid and specific detection of *Pseudomonas syringae* pv. morsprunorum races 1 and 2, using conventional and real-time PCR. *Applied microbiology and biotechnology*, 100(8), 3693-3711.
- Klevens, R. M., Morrison, M. A., Nadle, J., Petit, S., Gershman, K., Ray, S., & Active Bacterial Core surveillance (ABCs) MRSA Investigators. (2007). Invasive methicillin-resistant *Staphylococcus aureus* infections in the United States. *Jama*, 298(15), 1763-1771.
- Król, A., Pomastowski, P., Rafińska, K., Railean-Plugaru, V., & Buszewski, B. (2017). Zinc oxide nanoparticles: Synthesis, antiseptic activity and toxicity mechanism. *Advances in colloid and interface science*, 249, 37-52.
- Mahros, M. A., Abd-Elghany, S. M., & Sallam, K. I. (2021). Multidrug-, methicillin-, and vancomycin-resistant *Staphylococcus aureus* isolated from ready-to-eat meat sandwiches: An ongoing food and public health concern. *International Journal of Food Microbiology*, 346, 109165.
- McDonald, S., Prenzler, P. D., Antolovich, M., & Robards, K. (2001). Phenolic content and antioxidant activity of olive extracts. *Food chemistry*, 73(1), 73-84.
- Moghadam, E. T., Yazdani, M., Alam, M., Tebyanian, H., Tafazoli, A., Tahmasebi, E., & Seifalian, A. (2021). Current natural bioactive materials in bone and tooth regeneration in dentistry: a comprehensive overview. *Journal of Materials Research and Technology*, 13, 2078-2114.
- Motallaei, M. N., Yazdani, M., Tebyanian, H., Tahmasebi, E., Alam, M., Abbasi, K., & Yazdani, A. (2021). The current strategies in controlling oral diseases by herbal and chemical materials. *Evidence-Based Complementary and Alternative Medicine*, 2021(1), 3423001.
- Murthy, H. A., Desalegn, T., Kassa, M., Abebe, B., & Assefa, T. (2020). Synthesis of green copper nanoparticles using medicinal plant *Hagenia abyssinica* (Brace) JF. Gmel. leaf extract: Antimicrobial properties. *Journal of nanomaterials*, 2020(1), 3924081.
- Ordeghan, A. N., Khayatan, D., Saki, M. R., Alam, M., Abbasi, K., Shirvani, H., & Tebyanian, H. (2022). The wound healing effect of nanoclay, collagen, and tadalafil in diabetic rats: an in vivo study. *Advances in Materials Science and Engineering*, 2022(1), 9222003.
- Pérez-Alvarez, M., Cadenas-Pliego, G., Pérez-Camacho, O., Comparán-Padilla, V. E., Cabello-Alvarado, C. J., & Saucedo-Salazar, E. (2021). Green synthesis of copper nanoparticles using cotton. *Polymers*, 13(12), 1906.
- Rasigade, J. P., Dumitrescu, O., & Lina, G. (2014). New epidemiology of *Staphylococcus aureus* infections. *Clinical Microbiology and Infection*, 20(7), 587-588.
- Seidel, V., Peyfoon, E., Watson, D. G., & Fearnley, J. (2008). Comparative study of the antibacterial activity of propolis from different geographical and climatic zones. *Phytotherapy research*, 22(9), 1256-1263.
- Sudhakar, M., & Raman, B. V. (2020). Bactericidal and anti-biofilm activity of tannin fractions derived from *Azadirachta* against *Streptococcus mutans*. *Asian Journal of Applied Sciences*, 13, 132-143.
- Tong, S. Y., Davis, J. S., Eichenberger, E., Holland, T. L., & Fowler Jr, V. G. (2015). *Staphylococcus aureus* infections: epidemiology, pathophysiology, clinical manifestations, and management. *Clinical microbiology reviews*, 28(3), 603-661.



- Van Hal, S. J., Jensen, S. O., Vaska, V. L., Espedido, B. A., Paterson, D. L., & Gosbell, I. B. (2012). Predictors of mortality in *Staphylococcus aureus* bacteremia. *Clinical microbiology reviews*, 25(2), 362-386.
- Veiga, R. S., De Mendonça, S., Mendes, P. B., Paulino, N., Mimica, M. J., Lagareiro Netto, A. A., & Marcucci, M. C. (2017). Artepillin C and phenolic compounds responsible for antimicrobial and antioxidant activity of green propolis and *Baccharis dracunculifolia* DC. *Journal of applied microbiology*, 122(4), 911-920.
- Bakhshi, B., Sudhakar, M., & Lokesh, S. (2022). Garlic mediated green synthesis of silver nanoparticles as antifungal agents against *Magnaporthe oryzae*. *Indian Journal of Pharmaceutical Education and Research*, 56(4), 1245-1252.

